Application of a Fault Accommodation Approach to a Re-entry Vehicle

Andrés Marcos, Murray Kerr, Luis F. Peñín *

* *Deimos Space S.L., Ronda de Poniente VI, 28760 Madrid, Spain,*
{ *andres.marcos, murray.kerr, luis-felipe.penin*} *@deimos-space.com*

Abstract: In this paper a fault accommodation approach especially suitable for nonlinear dynamic inversion controllers is presented and applied to an atmospheric re-entry vehicle. The approach is based on the nominal/robustness decoupling principle used in recent high-performance architectures, reminiscent of anti-windup compensator approaches, and is well connected to the Youla-Kucera controller parameterizations used in the field of fault tolerant systems. The applicability of the approach is exemplified through its application to a high-fidelity nonlinear simulator of a reusable launch vehicle during re-entry which includes a nonlinear dynamic controller and an H-infinity based fault detection and isolation filter.

Keywords: Fault tolerant control, re-entry vehicles, nonlinear dynamic inversion.

1. INTRODUCTION

Nonlinear Dynamic Inversion (NDI) is a conceptually simple but powerful technique that has been used quite profusely in the last 15 years in the field of flight control (Honeywell and Lockheed Martin (1996); Vu, B.D. (1997)). In space its use is less prevalent but recently has been explored for atmospheric re-entry vehicles due to the challenging dynamics of this type of missions and the possibility of confronting them –throughout the complete re-entry corridor (Ito, D. et al. (2002); Da Costa, R.R. et al. (2003); Marcos, A. et al. (2007a)). It is well known that the main disadvantages of this technique is the numerical issues associated with the nonlinear inversion step and the lack of explicit robustness guarantees (Honeywell and Lockheed Martin (1996); Vu, B.D. (1997)). Indeed, it can be said that NDI addresses stability and performance, including robustness, through the use of other control synthesis techniques (Looye, G. and Joos, H.D. (2001); Papageorgiou, C. and Glover, K. (2005)).

Nowadays, and specially for automated atmospheric re-entry, the issue of fault tolerance has gained strong momentum. From this perspective, established control design techniques are being revisited in terms of their potential to absorb (i.e. accommodate or be-robust-to) faults while maintaining the fault-free nominal and robust stability/performance objectives. The standard industrial practice to address fault tolerance requirements is to use hardware redundancy (coupled with voting schemes) and/or banks of controllers (with banks of fault detection and isolation filters). These approaches are of course very valid but for space applications sometimes they are of limited use due to spacecrafts' weight budget and computational power constraints.

In this paper a fault accommodation approach, especially suited for NDI controllers, is presented. It uses the specific architecture of NDI controllers together a nominal/robustness decoupling principle that arises from recent high-performance architectures (Tay, T.T. et al. (1998); Zhou, K. and Ren, Z. (2001)). The application of the approach to a high-fidelity nonlinear simulation of a reusable launch vehicle (RLV) during the re-entry phase shows that the approach imbues the closed loop with fault tolerant control characteristics against actuator and sensor faults without requiring redesign of the baseline controller. It is highlighted that the current application stands out from other published FTC applications in that the designed FTC component uses the fault information from an industrially relevant FDI filter as opposed to idealized fault residuals.

The layout of the paper is as follows. Section 2 reviews the theoretical preliminaries of NDI control design and of high-performance control architectures. In Section 3 these concepts are used to developed the proposed fault accommodation approach. Section 4 describes the re-entry vehicle benchmark and presents the application of the approach.

2. THEORETICAL BACKGROUND

In this section the essential ideas behind NDI approaches and the concept of high-performance controller robustification are reviewed assuming an ideal system (no uncertainty, no disturbances and no faults) for clarity purposes. The exploitation of the synergies between both concepts is the key element of the proposed approach.

2.1 Nonlinear dynamic inversion

The NDI synthesis method considers a class of nonlinear systems affine in the control input. This last requirement is without loss of generality since it is always possible to transform a nonlinear input into a new affine input:

$$\begin{aligned} \dot{x} &= f(x) + g(x)u \\ y &= h(x) \end{aligned} \tag{1}$$

The state $f(x)$ and output $h(x)$ mappings are assumed smooth nonlinear functions of the states x while the input injection map $g(x)$ is assumed to be a diffeomorphism (a smooth function whose inverse exists and is also smooth). For simplicity of presentation only the state-input inversion will be treated in this article, i.e. $h(x) = x$.

Differentiating the output equation until the input signal appears yields:

$$\dot{y} = \dot{x} = f(x) + g(x)u \tag{2}$$

The required number of successive differentiations indicates the system's relative degree, which in this case is one. Furthermore, since this is a state-input problem there are no zero dynamics –an important consideration for NDI control synthesis, see Vu, B.D. (1997).

In order to define the NDI control law, a control task is chosen (e.g. tracking, regulation, etc) and its associated mathematical formulation is substituted in Equation 2. For example, choosing an error-minimization control objective $\nu = K(x_c - x)$ with K designed using any control technique leads to:

$$\dot{y}_{des} = \nu = K(x_c - x) = f(x) + g(x)u \tag{3}$$

Rearranging terms, the NDI control law u_{NDI} is:

$$u_{NDI} = g(x)^{-1}[-f(x) + K(x_c - x)] \tag{4}$$

Substitute this NDI control law in the system's state equation and simplify to get:

$$\dot{x} = f(x) + g(x)\Big(g(x)^{-1}[-f(x) + K(x_c - x)]\Big) = K(x_c - x) \tag{5}$$

Which assuming zero command for regulation, $y_c = x_c = 0$, yields the following linear closed loop:

$$\dot{y} = \dot{x} = -Kx = -Ky \;\Rightarrow\; \dot{y} + Ky = 0 \tag{6}$$

A graphical representation of a standard NDI controller architecture is given in Figure 1 where G_u represents the nominal system.

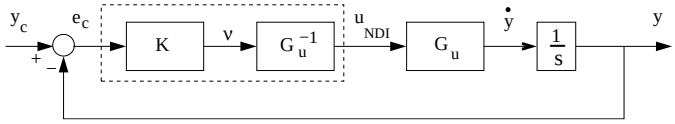

Fig. 1. Standard NDI controller structure.

It is highlighted that using the above standard NDI controller synthesis there is no direct fault accommodation design attempts. Therefore, unless the controller K has been designed to be highly robust to uncertainties and disturbances of large magnitude (which might include certain faults), the occurrence of faults will adversely affect the closed loop. Furthermore, the design of robust NDI controllers is still an open problem due to the dynamic inversion component of the approach. Thus, if an additional fault tolerance requirement is demanded, the design difficulty increases with likely poor or conservative results for the closed loop performance.

2.2 Robustification of high performance controllers

Before presenting the high-performance control architecture concept recall that the Youla parameterization provides a general parameterization of all stabilizing controllers for a given system in terms of a free, stable parameter $Q_c \in \Re H_\infty$ (the space of real, rational, proper and stable functions).

From (Zhou, K. et al. (1996)), let the system $G_u \in \Re H_P$ (the space of real-rational, and proper functions) and a stabilizing controller $K_o \in \Re H_P$ be given and assume they have the following right and left coprime factorizations:

$$\begin{aligned} G_u &= N_u M^{-1} = \tilde{M}^{-1}\tilde{N}_u \\ K_o &= UV^{-1} = \tilde{V}^{-1}\tilde{U} \end{aligned} \tag{7}$$

Where $N_u, M, \tilde{N}_u, \tilde{M}, U, V, \tilde{U}, \tilde{V} \in \Re H_\infty$ must satisfy the double coprime factorization:

$$\begin{bmatrix} \tilde{V} & -\tilde{U} \\ -\tilde{N}_u & \tilde{M} \end{bmatrix} \begin{bmatrix} M & U \\ N_u & V \end{bmatrix} = \begin{bmatrix} I & 0 \\ 0 & I \end{bmatrix} \tag{8}$$

The Youla parameterization represents the class of all proper controllers stabilizing the nominal plant $G_u \in \Re H_P$ as given by:

$$\begin{aligned} K(Q_c) =& (\tilde{V} + Q_c\tilde{N}_u)^{-1}(\tilde{U} + Q_c\tilde{M}) \\ =& K_o + \tilde{V}^{-1}Q_c(I + V^{-1}N_uQ_c)^{-1}V^{-1} \end{aligned} \tag{9}$$

for any $Q_c \in \Re H_\infty$ such that $\det(\tilde{V} + Q_c\tilde{N}_u)(\infty) \neq 0$ and $\det(I + V^{-1}N_uQ_c)(\infty) \neq 0$ are satisfied.

In reference Tay, T.T. et al. (1998), the above Youla parameterization is modified to obtain an architecture for high-performance controllers, see Figure 2. This architecture allows for a separation principle of the controller (represented by $K_o = \tilde{V}^{-1}\tilde{U}$ and Q_c) that has the potential to address the trade-off between nominal and robust performance objectives.

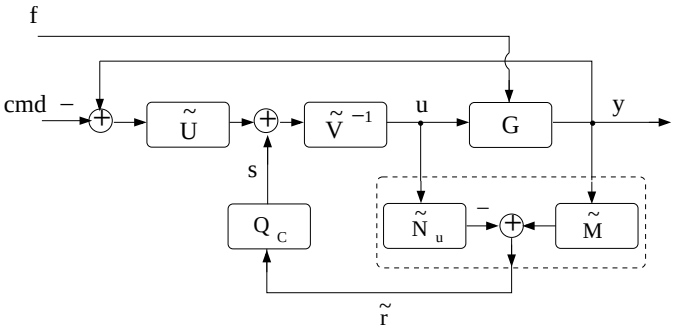

Fig. 2. High-performance control architecture.

The controller structure given in Figure 2 can be interpreted from a robustification perspective as follows. Let $K_o = \tilde{V}^{-1}\tilde{U}$ be a high-performance stabilizing controller for the nominal system G obtained by any control synthesis technique (e.g. classical, optimal, or modern). The Youla parameter Q_c can then be viewed as a robustifying controller that only takes action in the feedback loop whenever exogenous signals or model uncertainties are present, i.e. when the primary residual $\tilde{r}$ is non-zero.

It is straightforward to connect the above architecture to FDI and FTC designs. Indeed, it is seen from Figure 2 that the primary residual represents an estimate of the fault effects on the system when faults are introduced, if $y = G_u u + G_f f$ then:

$$\tilde{r} = \tilde{M}y - \tilde{N}_u u = \tilde{M}(\tilde{M}^{-1}\tilde{N}_u u + \tilde{M}^{-1}\tilde{N}_f f) - \tilde{N}_u u = \tilde{N}_f f \tag{10}$$

And the controller input u in Figure 2 is then given by:

$$u = \tilde{V}^{-1}[\tilde{U}(y_c - y) + Q_c\tilde{r}] = K_o(y_c - y) + \tilde{V}^{-1}Q_c\tilde{N}_f f \tag{11}$$

Substituting u into the faulty system $y = G_u u + G_f f$ yields:

$$\begin{aligned} y =& G_u[K_o(y_c - y) + \tilde{V}^{-1}Q_c\tilde{N}_f f] + G_f f \\ =& G_uK_o(y_c - y) + \tilde{M}^{-1}(\tilde{N}_u\tilde{V}^{-1}Q_c + 1)\tilde{N}_f f \end{aligned} \tag{12}$$

Therefore, in order to cancel the fault effects on the closed loop the fault compensator Q_c should be equal (or rather an approximation at the frequency regions of interest) to:

$$Q_c = -\tilde{V}\tilde{N}_u^{-1} \tag{13}$$

Note that if this ideal Q_c (no sensor/actuator dynamics nor uncertainty are considered) is substituted into the Youla parameterization in Equation 9, an infinite gain controller is obtained.

This means asymptotically perfect disturbance (or fault) rejection, i.e. zero sensitivity at the disturbance frequencies. Nevertheless, this is not desirable due to the physical impossibility of implementing infinite controllers for example.

3. FAULT TOLERANT NDI CONTROL DESIGN

As aforementioned, the proposed NDI fault accommodation approach is an extension of the previous fault robustification architecture to NDI control. Indeed, the previous architecture does not restrict itself to NDI controllers (Zhou, K. and Ren, Z. (2001); Marcos, A. et al. (2007b)) but this extension provides for a methodology that takes advantage of the characteristics of NDI controllers (their conceptual simplicity and cross-platform applicability) while imbuing the design with active fault tolerance properties. It is also a very useful approach for retrofitting purposes, where an already designed NDI controller is required to be upgraded for fault tolerance purposes but avoiding costly re-design steps.

A simple, but revealing, graphical representation of the proposed approach is obtained combining Figures 1 and 2, see Figure 3:

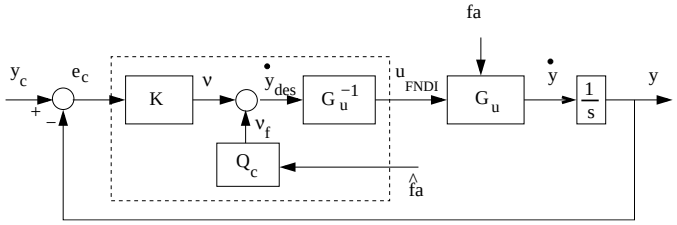

Fig. 3. Fault accommodated NDI controller.

Note that the fault robustification parameter Q_c uses an estimate of the fault $\hat{f}_a$ (typically available from a FDI component). This fault estimate can be considered as a residual signal since it should be equal to zero if no fault is present and different to zero otherwise (equivalent to the primary residual signal in the previous section), $\hat{f}_a = \tilde{r} = \tilde{N}_f f$.

The objective is to design the compensator Q_c such that: (i) the addition of the signal ν_f to the signal ν results in fault-free, or gracefully degraded, desired rate behavior under the occurrence of a fault; and (ii) minimally degrades the closed-loop under fault-free conditions. Note that these conditions are similar to those found in anti-windup schemes, and that approaches for robust anti-windup of recent appearance have been based on the high-performance architecture Marcos, A. et al. (2007b).

The proposed fault robustification NDI approach is formalized as follows. From the faulty system given by Equation 14:

$$\begin{aligned} \dot{x} &= f(x) + g(x)(u + f_a) \\ y &= x \end{aligned} \tag{14}$$

Subsequently, choose the nominal control task ν and include the fault compensation signal $\nu_f = Q_c \hat{f}_a$:

$$\dot{y}_{des} = \nu + \nu_f = K(y_c - y) + Q_c \hat{f}_a = f(x) + g(x)u \tag{15}$$

The fault compensated NDI control law u_{FNDI} can then be obtained:

$$u_{FNDI} = g(x)^{-1}[-f(x) + K(y_c - y) + Q_c \hat{f}_a] \tag{16}$$

To obtain design insight on the fault compensator Q_c, substitute the above u_{FNDI} into the faulty system of equation 14 to obtain:

$$\begin{aligned} \dot{x} &= f(x) + g(x)\left(g(x)^{-1}[-f(x) + K(y_c - y) + Q_c \hat{f}_a]\right) \\ &\quad + g(x) f_a = K(y_c - y) + g(x)[g(x)^{-1} Q_c \hat{f}_a + f_a] \end{aligned} \tag{17}$$

From where, assuming that the fault estimate $\hat{f}_a$ is approximately equal to the fault, it is obtained that selecting $Q_c = -g(x)$ will cancel the effects of the fault in the linear closed loop:

$$\dot{y} = K(y_c - y) + g(x)[I + g(x)^{-1} Q_c] f_a = K(y_c - y) \tag{18}$$

Remark 1. The selection of Q_c given above is based on a perfect identification of the fault and perfect knowledge of the input component of the system. In practice, Q_c needs to be designed for both: (i) compensation of the fault effects on the internal control signal u and (ii) to compensate imperfect fault estimation (that is, assuming that uncertainty and command decoupling objectives for the FDI system were only partially achieved).

Remark 2. Although the second objective of Q_c seems stringent, it is not so since it is assumed that the quality of the estimated fault is *at least in the (frequency) regions of interest* fairly acceptable. This assumption reflects the fact that current FDI techniques can detect and identify faults with considerable accuracy. In any case, Q_c represents an additional degree-of-freedom that can be used to compensate for limitations of the FDI component.

Remark 3. The above parameter $Q_c = -g(x)\hat{f}_a$ and that from Equation 13 ($-\tilde{V}\tilde{N}_u^{-1}\tilde{r}$) share the same role. To show this, redraw the architecture from Figure 2 combining the nominal controller $K_o = \tilde{V}^{-1}\tilde{U}$ and shifting the signal s to the plant input so that Q_c becomes now $-\tilde{N}_u^{-1}$ as shown in Figure 4.

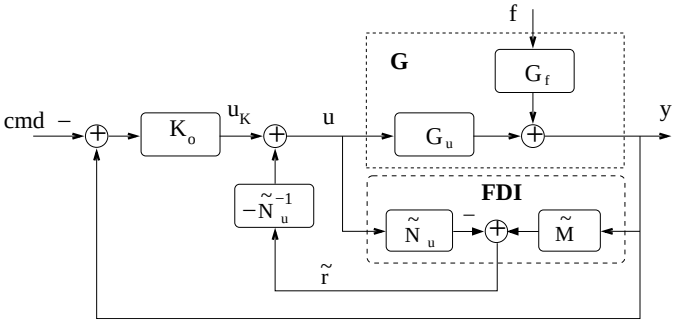

Fig. 4. High-performance control architecture (redrawn).

From this new representation, it can be concluded that Q_c is trying to invert the input injection map dynamics $g(x) = \tilde{N}_u$ so that the primary residual $\hat{r}$ cancels the fault effects:

$$\begin{aligned} y &= \tilde{M}^{-1}\tilde{N}_f f + \tilde{M}^{-1}\tilde{N}_u[u_K - \tilde{N}_u^{-1}\tilde{r}] \\ &\text{thus } \tilde{M}^{-1}\tilde{N}_f f - \tilde{M}^{-1}\tilde{r} = 0 \;\Rightarrow\; y = G_u u_K \end{aligned} \tag{19}$$

The advantage is that since it is used within the NDI controller configuration there is no need for the inversion (taken care of automatically by the design of the baseline NDI system).

Moreover, Q_c was previously set equal to $-g(x)$ only because it was assumed an additive actuator fault, i.e. $g(x)[u + fa]$. More general representations (accounting also for sensor and/or parametric faults) can be easily obtained assuming the system is given by:

$$\begin{aligned} \dot{x} &= f(x) + g(x)u + l(x)f \\ y &= x \end{aligned} \tag{20}$$

Where $l(x)$ is a smooth map representing the fault signature. In this manner, the fault-accommodation parameter is now given by $Q_c = -l(x)$ (if the same fault estimate assumption as before is used, i.e. perfect identification). In essence, the resulting architecture can be construed as a "virtual actuator" (when the faults considered are in actuator system) or as a post-controller implemented "virtual sensor" (when the faults are from the sensor system).

Remark 4. Indeed, note that the fault compensation signal ν_f can be added after the system dynamics inversion, block G_u^{-1} in Figure 3, in the case of actuator faults or before the input to the controller K in the case of sensor faults. In the former case, the following NDI control law is obtained:

$$\bar{u}_{FNDI} = g(x)^{-1}[-f(x) + K(x_c - x)] + Q_c \hat{f}_a \tag{21}$$

Which results in the free-parameter $Q_c = -g^{-1}(x)l(x)$ when substituted in the general case from Equation 20 as seen below:

$$\begin{aligned} \dot{x} = f(x) + g(x)g(x)^{-1}[-f(x) + K(y_c - y)] \\ + g(x)Q_c \hat{f}_a + l(x) f_a \end{aligned} \tag{22}$$

The sensor case possibility is referred to in the community as "virtual sensor", as it corrects sensor anomalies by means of analytical redundancy. In any case, and as seen in Equation 22 the success of the compensation will depend on how well the term $g(x)Q_c \hat{f}_a$ cancels the term $l(x) f_a$ –note that sensor faults can be represented as pseudo-actuator faults by augmenting the system with additional states, and thus it fits the general case above. Nevertheless, for inversion-based controllers it is better to compensate the faults before the dynamic inversion: based on the fact that the desired commanded input variation to the inversion block, $\dot{y}_{des}$, should be typically equal to zero except for transient behaviour Honeywell and Lockheed Martin (1996), which for a fault-uncompensated measured output will not be the case. And also, to avoid saturation of the control signal – a critical phenomenon for NDI controllers typically addressed after the dynamic inversion through the so-called control allocation or control hedging schemes Honeywell and Lockheed Martin (1996); Ito, D. et al. (2002).

4. APPLICATION TO A RE-ENTRY VEHICLE

4.1 Hopper reusable launch vehicle

The Hopper, see figure 5, is a horizontally launch and landing rocket-propelled vehicle comprising a reusable primary stage, the RLV Hopper and one expendable upper stage. It executes sub-orbital point-to-point flights of around 30 minutes. A typical profile mission comprises acceleration to prescribed sub-orbital staging conditions, cargo ejection, drift to 150 km altitude, automated re-entry, and gliding to one of its dedicated landing sites some 4500 km downrange launch-site, depending on mission inclination. The aerodynamic configuration features a compact body with rounded edge-like cross section equipped with a delta wing far rear and a central vertical tail. The tapered delta wing has 60^o leading edge sweep, slightly swept back hinge lines of elevons, and slightly sweptback trailing edge.

The aerodynamic controls comprise rudders on the vertical tail capable of $\pm\ 30^o$ symmetric deflection range, inboard and outboard elevons on the wings with symmetric deflection range of $\pm\ 20^o$ and $\pm\ 25^o$ respectively, a fairly large body flap (range of $[-15^o \quad +25^o]$) underneath the main engines, and speed brakes $[0^o \quad +85^o]$ left and right on the engine bay. The inboard

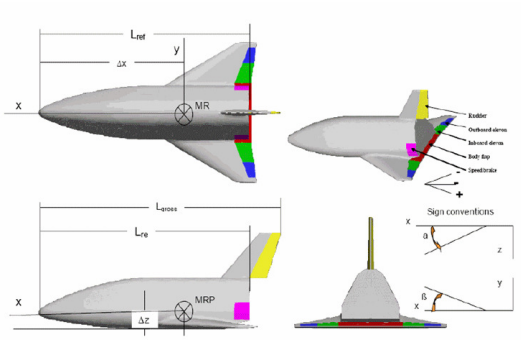

Fig. 5. Hopper 4-view profile.

and outboard elevons combine the left and right surfaces to form eleron and aileron deflections, furthermore, the inboard surfaces are used predominantly for trim while the outboard for flying. A reaction control system (RCS) is needed to orient and stabilize the vehicle during stage separation, to counteract MECO injection dispersions, and to bring the vehicle into the attitude required for entry. The RCS is composed of four clusters (each with 3-thrusters) located in the left and right side of the vehicle's front and rear.

The Hopper high-fidelity aerodynamic database was provided by Astrium Space Transportation (Bremen, Germany) and consists of nonlinear look-up tables (LUT) dependent on angle of attack, Mach number, sideslip, altitude and the control effectors. Each LUT provides an estimate of the principal stability derivatives and they can be grouped into non-effector and effector-dependent contributors of the aerodynamic coefficients. Furthermore, the database is divided into hypersonic and supersonic/sub-sonic datasets bridged together during a transition phase scheduled on Mach number. The aerodynamic database is embedded in a nonlinear high-fidelity Matlab/Simulink simulator with full nonlinear equations of motion, 1962 USSA atmospheric model, ellipsoidal planet shape, time delays, noise, colored sensor models and 2nd order actuator models with magnitude and rate saturations Marcos, A. et al. (2007a).

4.2 Baseline NDI controller

A re-entry inner-loop control design was developed for the Hopper vehicle in reference Marcos, A. et al. (2007a). The NDI approach used is characterized by: (i) A four step-approach with a mixed Wind/Body-axes formulation, which is closer to NDI designs for aircraft and is more amenable to tuning as it decouples the motion of the three axes and can be motivated better from a flight mechanics perspective; (ii) a moment allocation scheme that automates the transitions for the different flight phases based on dynamic pressure and Mach; And (iii), the "pure" inversion step which uses a decoupling approach based on *flight* and *trim* surface calculations applicable due to the Hopper's actuation redundancy.

The NDI controller calculates the necessary effector deflections, RCS and aerosurfaces δ's, based on reference aerodynamic angles: angle of attack α_{ref}, sideslip angle β_{ref} and bank angle σ_{ref}. The control design objectives consist in accurate tracking of the reference angles and avoidance of control effector saturation in the face of parametric and aerodynamic uncertainties.

The parametric uncertainty arises due to the imperfect knowledge for some critical parameters, e.g. vehicle mass, while the aerodynamic mismatch is introduced to recreate the uncertainty that exists in knowing the aerodynamic database (intrinsically very difficult to identify) and to avoid perfect cancellation of the dynamics implemented in the simulator due to the controller inversion. Mach-based percentage changes are applied to the aerodynamic coefficients calculations, together with correlation of the lift (L) and drag (D) calculations based on the L/D ratio, in order to more realistically simulate the uncertain conditions.

4.3 $\mathcal{H}_\infty$ fault detection and isolation filters

In reference Kerr, M. et al. (2008), a gain-scheduled $\mathcal{H}_\infty$ FDI filter for rudder actuator and sideslip sensor faults is designed and validated in the same simulator as above. This fault set was chosen because both faults strongly affect the vehicle lateral/directional motion in a similar manner, making the FDI problem quite challenging: the rudder is the main lateral effector while the sideslip is one of the main lateral sensors. As is not assumed that these faults act in a mutually independent manner, the FDI filter must be designed to simultaneously detect faults in the rudder actuator and sideslip sensor and ensure that such faults do not have a significant adverse effect on the fault detection capabilities for the other channel.

Initially, a total of 19 LTI FDI filters were designed along the flight trajectory but it was readily observed that the point-design FDI filters had limited performance/robustness properties when applied at trim points away from that for which they were designed. Thus, a scheduling of a subset of the point-design LTI FDI filters was performed to improve the FDI robustness to parameter variations. Three point-design LTI FDI filters were chosen over a 90 second flight period of interest and scheduled using a quadratic scheduling law dependent on time. As described in reference Kerr, M. et al. (2008), the FDI filter performs quite well in decoupling and estimating the faults – even in a Monte Carlo setting.

4.4 Fault tolerant control design and results

The design of the fault compensators is performed in a heuristically manner, but it is noted that convergence to an acceptable $Q_f = diag(Q_{f_{act}}, Q_{f_{sen}})$ was quick and straight forward. The accommodation signal from each compensator is summed to the desired sideslip rate within the NDI controller, as it is the main lateral/directional state affected by the selected faults, and prior to any system inversion. For the rudder actuator fault, the selected compensator is given by $Q_{f_{act}} = \frac{-0.01}{s+0.7}$ and is driven by the rudder residual from the aforementioned gain-scheduled $\mathcal{H}_\infty$ FDI filter, while for the sideslip sensor fault, the designed fault compensator is equal to $Q_{f_{sen}} = \frac{0.7}{s+0.7} * K_{PID_\beta}$ and is driven by the sensor fault FDI residual.

Figure 6 shows the tested actuator fault and the FDI fault residual signals while Figure 9 that for the sensor case.

Figure 7 presents the rotational states' comparison between (a) the no-fault, (b) the fault without Q_f and (c) the fault with Q_f cases for the rudder actuator fault. A small improvement is observed with respect to the sideslip tracking. The rest of the states suffer no distinguishable difference despite the strength of the fault (10 degrees of rudder bias). The small fault effect is the result of the natural fault tolerant properties of the NDI controller from reference Marcos, A. et al. (2007a), which for actuator fault results in automatic compensation due to the Hopper's aerodynamic surfaces redundancy. For example, observe the equal but different sign deflections of the right and left outboard electro-mechanical-actuators (EMA) in Figure 8 – the fault cases with and without compensator are almost exactly overlaid.

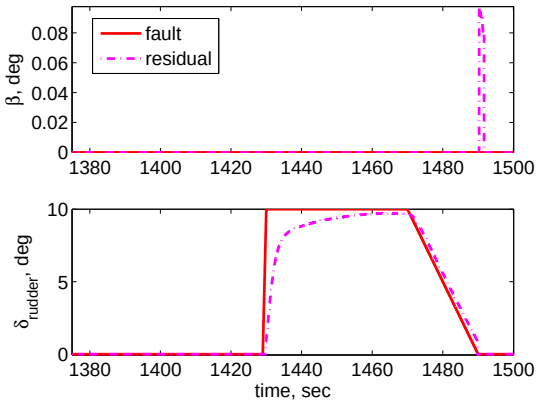

Fig. 6. Actuator fault: fault versus FDI fault signals.

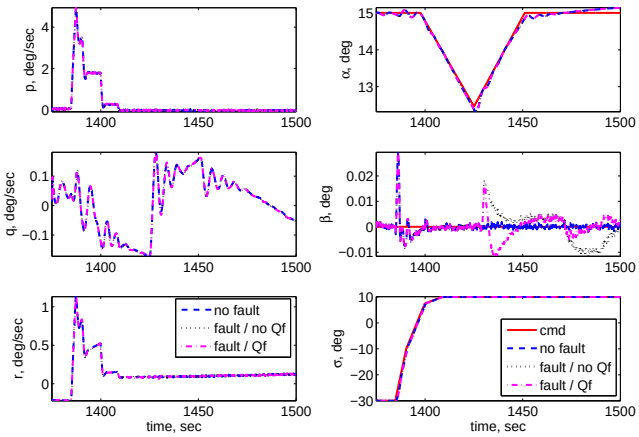

Fig. 7. Actuator fault: state comparison.

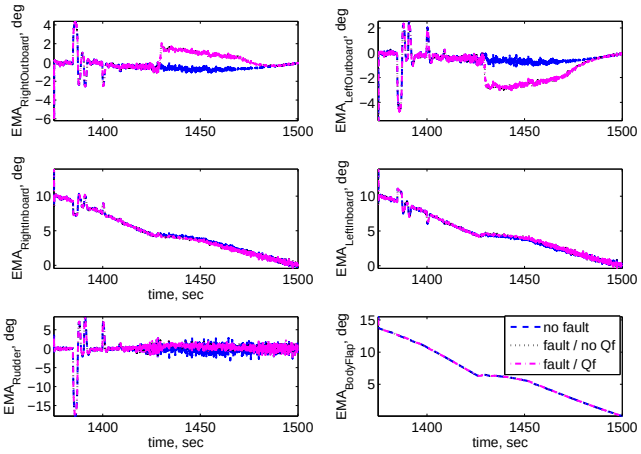

Fig. 8. Actuator fault: deflection comparison.

For the sideslip sensor fault case, the fault benefits are much clearer. Looking at the state responses, Figure 10, it is noticeable a quite improved sideslip tracking. Further, in this case the correction of the desired rate prior to the system dynamic inversion has the additional benefit of ameliorating the use of the actuators. This is observed in Figure 11 were only for the case of the fault without Q_f there are opposite and cancelling deflections for the outboard and inboard EMAs and a relatively strong (around 5 degrees) deflection of the rudder during the fault occurrence.

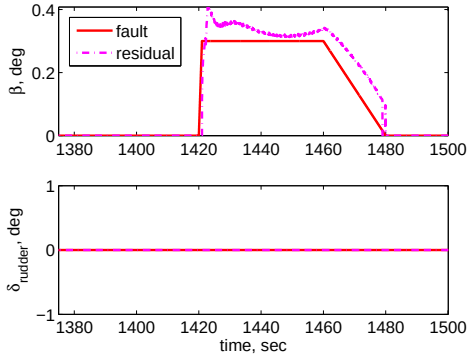

Fig. 9. Sensor fault: fault versus FDI fault signals..

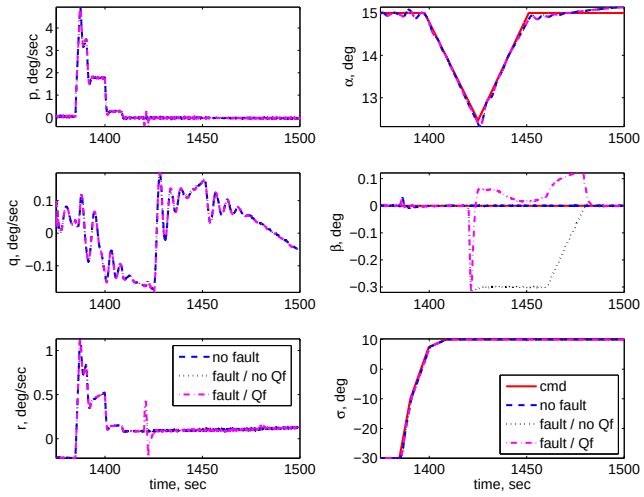

Fig. 10. Sensor fault: state comparison.

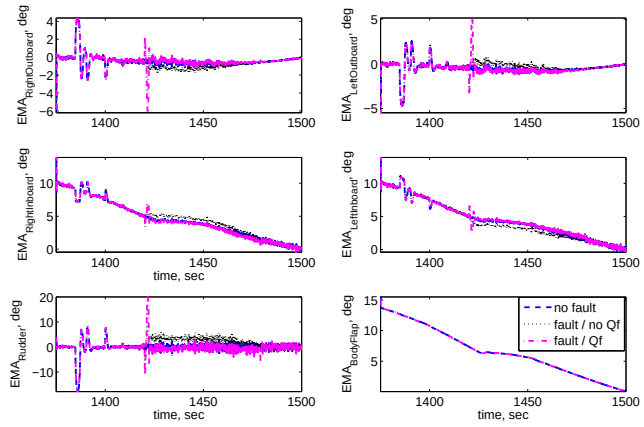

Fig. 11. Sensor fault: deflection comparison.

5. CONCLUSION

In this paper a fault accommodation approach for NDI controllers has been presented and applied to a reusable launch vehicle during the re-entry phase. The approach extends to NDI controllers a recent robustification concept used for high-performance controllers. This extension takes advantage of the natural characteristics of NDI controllers (mainly the separation of the controller into an inversion of the dynamics and a control law computation) to imbue the closed loop with fault tolerance characteristics in a very straightforward manner. The results of the application show that the approach has the potential to imbue the closed loop design with fault tolerant characteristics without necessitating redesign of the baseline controller.

ACKNOWLEDGEMENTS

The authors wish to express their gratitude to Josef Sommer and Wolfgang Belau from Astrium Space Transportation (Bremen, Germany) for their support with the Hopper RLV.

REFERENCES

Da Costa, R.R., Chu, Q.P., and Mulder, J.A. (2003). Re-entry Flight Controller Design Using Nonlinear Dynamic Inversion. *Journal of Spacecraft and Rockets*, 40(1).

Honeywell and Lockheed Martin (1996). Application of Multivariable Control Theory to Aircraft Control Laws. Technical Report WL-TR-96-3099, Flight Dynamics Directorate, Wright Laboratory, Wright-Patterson Air Force Base, OH.

Ito, D., Georgie, J., Valasek, J., and Ward, D.ST (2002). Re-entry Vehicle Flight Controls Design Guidelines: Dynamic Inversion. Technical Report NASA/TP-2002-210771, Flight Simulation Laboratory, Texas A&M University.

Kerr, M., Marcos, A., Penin, L.F., and Bornschlegl, E. (2008). Gain-scheduled fdi for a re-entry vehicle. In *AIAA Guidance, Navigation, and Control Conference*. Hawaii, USA.

Looye, G. and Joos, H.D. (2001). Design of Robust Dynamic Inversion Control Laws using Multi-Objective Optimization. In *AIAA Guidance, Navigation, and Control Conference*. Montreal, Canada.

Marcos, A., Peñín, L.F., Caramagno, A., Sommer, J., Belau, W., and Bornschlegel, E. (2007a). Design of a fully automated NDI attitude controller for the Hopper atmospheric re-entry. In *17th Conference on Automatic Control in Aerospace*. Toulouse, FR.

Marcos, A., Turner, M.C., and Postlethwaite, I. (2007b). An architecture for design and analysis of high-performance robust anti-windup compensators. *IEEE Transactions on Automatic Control*, 52(9).

Papageorgiou, C. and Glover, K. (2005). Robustness Analysis of Nonlinear Flight Controllers. *Journal of Guidance, Control, and Dynamics*, 28(4), 639–648.

Tay, T.T., Mareels, I., and Moore, J.B. (1998). *High Performance Control*. Birkhauser.

Vu, B.D. (1997). Nonlinear Dynamic Inversion Control. In Magni, J.F., Bennani, S., and Terlouw, J. (eds.), *Robust Flight Control: A Design Challenge*, chapter 9. Springer-Verlag. Lecture Notes in Control and Information Sciences.

Zhou, K., Doyle, J.C., and Glover, K. (1996). *Robust and Optimal Control*. Prenticel-Hall, Englewood Cliffs, NJ.

Zhou, K. and Ren, Z. (2001). A New Controller Architecture for High Performance, Robust, and Fault-Tolerant Control. *IEEE Transactions on Automatic Control*, 46(10), 1613–1618.